

1 **Control flow in active inference systems**

2 **Part II:**

3 **Tensor networks as general models of control**

4 **flow**

5 Chris Fields^{a,*}, Filippo Fabrocini^{b,c}, Karl Friston^{d,e}, James F. Glazebrook^{f,g},
Hananel Hazan^a, Michael Levin^{a,h} and Antonino Marcianò^{i,j,k}

^a *Allen Discovery Center at Tufts University, Medford, MA 02155 USA*

^b *College of Design and Innovation, Tongji University, 281 Fuxin Rd,
200092 Shanghai, CHINA*

^c *Institute for Computing Applications “Mario Picone”,
Italy National Research Council, Via dei Taurini, 19, 00185 Rome, ITALY*

^d *Wellcome Centre for Human Neuroimaging, University College London,
London, WC1N 3AR, UK*

^e *VERSES Research Lab, Los Angeles, CA, 90016 USA*

^f *Department of Mathematics and Computer Science,
Eastern Illinois University, Charleston, IL 61920 USA*

^g *Adjunct Faculty, Department of Mathematics,
University of Illinois at Urbana-Champaign, Urbana, IL 61801 USA*

^h *Wyss Institute for Biologically Inspired Engineering at Harvard University,
Boston, MA 02115, USA*

ⁱ *Center for Field Theory and Particle Physics & Department of Physics
Fudan University, Shanghai, CHINA*

^j *Laboratori Nazionali di Frascati INFN, Frascati (Rome), ITALY*

^k *INFN sezione Roma “Tor Vergata”, I-00133 Rome, ITALY*

7 **Abstract**

8 Living systems face both environmental complexity and limited access to free-energy re-
9 sources. Survival under these conditions requires a control system that can activate, or
10 deploy, available perception and action resources in a context specific way. In the accompa-
11 nying Part I, we introduced the free-energy principle (FEP) and the idea of active inference
12 as Bayesian prediction-error minimization, and show how the control problem arises in ac-
13 tive inference systems. We then reviewed classical and quantum formulations of the FEP,
14 with the former being the classical limit of the latter. In this Part II, we show that when
15 systems are described as executing active inference driven by the FEP, their control flow
16 systems can always be represented as tensor networks (TNs). We show how TNs as control
17 systems can be implemented within the general framework of quantum topological neural
18 networks, and discuss the implications of these results for modeling biological systems at
19 multiple scales.

20

21 **Keywords**

22 Bayesian mechanics; Dynamic attractor; Free-energy principle; Quantum reference frame;
23 Scale-free model; Topological quantum field theory

24

25 **1 Introduction**

26 The framework of *active inference* provides a completely general, scale-free formal frame-
27 work for describing interactions between physical systems in cognitive terms. In Part I of

*Corresponding author at: Allen Discovery Center at Tufts University, Medford, MA 02155 USA; *E-mail address:* fieldsres@gmail.com

28 this paper, we reviewed how active inference – a combination of learning with active explo-
29 ration of the environment – emerges in systems compliant with the Free Energy Principle
30 (FEP), a general least-action principle initially developed in neuroscience [1, 2, 3, 4, 5, 6, 7].
31 We then showed how the control flow problem arises in active inference systems, and re-
32 viewed classical and quantum formulations of the problem. Control flow can be represented
33 as switching between classical dynamical attractors, between deployed quantum reference
34 frames (QRFs) [8, 9], and between computational processes represented by TQFTs [10, 11].
35 Implementing control flow has a free-energy cost; hence any control-flow system must trade
36 off its own processing costs against the expected benefits of switching between input/output
37 modes. The time and memory dependence of control flow generically leads to context effects
38 on both perception and action.

39 In this Part II, we develop a fully-general tensor representation of control flow in §2, and
40 prove that this tensor can be factored into a TN if, and only if, the separability (or condi-
41 tional statistical independence) conditions needed to identify distinct features of, or objects
42 in, the environment are met. We show how TN architectures allows classification of control
43 flows, and give two illustrative examples. We then discuss several established relationships
44 between TNs and artificial neural network (ANN) architectures in §3, and show how these
45 generalize to topological quantum neural networks [11, 12], of which standard deep-learning
46 (DL) architectures are a classical limit [13]. Having developed these formal results, we turn
47 to implications of these results for biology in §4, and discuss how TN architecture correlates
48 with the observational capabilities of the system being modeled, particularly as regards abil-
49 ities to detect spatial locality and mereology. We consider how to classify known control
50 pathways in terms of TN architecture and how to employ the TN representation of control
51 flow in experimental design. We conclude by looking forward to how these FEP-based tools
52 can further integrate the physical and life sciences.

2 Tensor network representation of control flow

2.1 Tensor networks and holographic duality

Entanglement and quantum error correction, two concepts developed in quantum information theory, have been proved to have a fundamental role in unveiling quantum gravity [14]. At the origin of this consideration is the discovery by Bekenstein and Hawking [15, 16, 17, 18] that the second law of thermodynamics can be preserved in the gravitational field of a black hole, if this latter has an entropy proportional to the area of its horizon, by the inverse of the Newton gravitational constant G . This entropy is maximal, as implied by the second law itself, providing an upper bound for possible configurations of matter within a region of the same size [19, 20].

Nonetheless, the scaling of the local degrees of freedom counted by the entropy does not increase as the volume, hinging toward the formulation of the holographic conjecture [21], suggesting a division between the information that can only be retrieved on the boundary world, and a merely apparent bulk world. AdS/CFT realized the holographic conjecture, postulating a duality between gravity in asymptotically AdS space and quantum field theory on the spatial infinity of the AdS space [22]. Giving literal meaning to the duality, Ryu and Takayanagi (RT, [23]) proposed that entanglement of a boundary region fulfils the same law as for the black hole entropy, replacing the area of the black hole horizon with an extremal surface area that bounds the bulk region under scrutiny.

While on the boundaries the theory can be individuated by assigning a specific conformal field theory (CFT), in the bulk the geometry can be associated to specific entanglement structures of the quantum systems. This is, for instance, what happens to the ground states of a CFT associated to an AdS space: the RT surface area increases less fast than the volume of the boundary. When the boundary is at equilibrium, in a thermal state of

77 finite temperature, the bulk geometry corresponds to that of a black hole, its horizon being
78 parallel to the boundary and its size increasing with the temperature. The RT surface is
79 then confined between the boundary and the black hole horizon, approaching the boundary
80 at higher temperature and increasing its entropy. These considerations suggest the existence
81 of a subtle link interconnecting the structure of spacetime and quantum entanglement, and
82 hence that a theory of quantum gravity must be fundamentally holographic, where its states
83 satisfy the RT formula for some bulk geometry.

84 The existence of an exact correspondence between bulk gravity and quantum theory at the
85 boundary may hinge toward possible inconsistencies with locality. This has been discussed
86 in the literature, in terms of local reconstruction theory [24, 25, 26]: variables in the bulk
87 (e.g. bulk spins) can be controlled instantaneously from the boundary, but this requires
88 simultaneous access to a large portion of the boundary: locality and an upper speed of
89 light do not hold exactly in this theory. Nonetheless, local observers confined in small
90 regions at the boundary still fulfill locality and the existence of an upper limit of the speed
91 of information exchange, in a way that is reminiscent of quantum error correction codes
92 (QECCs) in quantum information theory: information is stored redundantly, in such a way
93 that when part of it is corrupted, a reconstruction of information is still possible. Locality
94 in the bulk is therefore a QECC property of the encoding map that realizes the duality
95 between bulk and boundary. On the other hand, these properties are strictly connected to
96 RT, which provides the necessary resource of entanglement for QECC to emerge [27].

97 The RT formula and QECC are properties fulfilled by different classes of models, among
98 which TNs [28]. These have been first introduced in condensed matter physics as variational
99 wave-functions of strongly correlated systems [29, 30]. TNs are many-body wavefunctions
100 that can be derived by composing few-body quantum states, which are indeed tensors. A
101 prototype TN is, e.g., a collection of Einstein-Podolsky-Rosen (EPR) entangled pairs of
102 qubits: in a nonentangled basis, the measured qubits are in some entangled pure state,

103 and can be composed with additional qubits to create states with increasing complexity.
104 Indeed, complicated quantum entanglement can be derived by entangling only a few qubits
105 [31].

106 Particularly relevant for its implications on the reconstruction of spacetime structure is the
107 multi-scale entanglement renormalization ansatz (MERA) [32]. TNs can be naturally re-
108 lated to holography duality by considering that their entanglement entropy can be controlled
109 by their graph geometry. Some versions of TNs that are characterized by RT entanglement
110 entropy and QEEC have been constructed resorting to stabilizer codes [33, 34] and random
111 tensors with large bond dimensions [35]. TNs with random tensors at each node can be
112 regarded as random states restricted by the topology of the network. Exactly as random
113 states are almost maximally entangled, random TNs show, through the RT formula, an
114 almost maximal entanglement, providing a large family of states with interesting proper-
115 ties to explore holographic duality. Furthermore, for random TNs, the RT formula holds
116 in generic spaces with not necessarily hyperbolic geometry, hinging toward an extension
117 of holographic duality beyond AdS, to more general configurations in quantum gravity.
118 Nonetheless, at least in three dimensions, random tensor networks have been related to the
119 gravitational action, by means of the Regge calculus [36].

120 On the other hand, since geometry emerges as a specification of the entanglement structure,
121 one may consider that the Einstein equations should be connected as well to the dynamics of
122 entanglement. For small perturbations around the ground state of a CFT on a boundary,
123 linearized Einstein equations have been derived from the RT formula [37, 38]. Indeed,
124 the conformal symmetry enables a relationship between the energy-momentum and the
125 entanglement entropy, and consequently the area of the extremal surface can be connected
126 to the energy-momentum distribution at the boundary – the result is equivalent to the
127 linearized Einstein equations.

128 The dynamics on the boundary, on the other hand, shows a chaotic behaviour, with scram-

129 bling of the single-particle operators, which evolve into multi-particle operators [39]. Maxi-
130 mal chaotic behavior recovered in the growth of the commutator between ladder operators,
131 as encoded in the out-of-time-ordered correlation (OTOC) functions, is characterized by
132 exponential growth in time and temperature. A model endowed with this property is, e.g.,
133 the Sachdev-Ye-Kitaev model, developed to describe certain systems in condensed matter
134 physics, such as Gapless spin-fluids [40, 41, 42]. On the other hand, operator scrambling is
135 also related to QEEC: the chaotic dynamics at the boundary instantiates QECC preserv-
136 ing quantum information, which is efficiently hidden (and protected) behind the horizon.
137 Nevertheless, this has led to many questions concerning the information behind the horizon
138 being eventually accessible from the boundary through non-local measurements, the fate of
139 the local degrees of freedom hitting the singularity, and the relation between the causal
140 structure of the bulk and the smooth geometry across the horizon.

141 2.2 General results

142 We can now move to prove a general result:

143 **Theorem 1.** *A system A exhibits non-trivial control flow if, and only if, its control flow*
144 *can be represented by a TN.*

145 and examine some of its corollaries. We begin by defining:

146 **Definition 1.** *Control flow is trivial if a system deploys only one QRF.*

147 As any collection of mutually-commuting QRFs can be represented as a single QRF [11, 79],
148 any system that deploys only mutually-commuting QRFs exhibits trivial control flow.

149 Systems that deploy only a single QRF “do the same thing” regardless of context, and so do
150 not qualify as “interesting” in the sense used here. As noted above, no finite physical system
151 can measure the entire state of its boundary with a single QRF, so no such system can

152 simultaneously measure and act on its entire context. Any system A that deploys multiple
 153 QRFs Q_i in sequence cannot, as noted in Part I, avoid contextuality due to unobservable
 154 effects, mediated by the action of H_B , of the action of Q_i on the state later measured by
 155 Q_j . Every action taken by an “interesting” system, in other words, at least transiently
 156 increases the VFE at its boundary.

157 Consider, then, a system A that deploys multiple, distinct QRFs Q_1, Q_2, \dots, Q_n acting on
 158 its environment B , where $n \ll N = \dim(H_{AB})$. Classical control flow in A can then be
 159 represented by a matrix $\mathbf{CF} = [P_{ij}]$, where P_{ij} is the probability of the control transition
 160 $Q_i \rightarrow Q_j$. As noted in Part I, any such transition has an energetic cost, which must be
 161 paid with free energy sourced from the thermodynamic sector F of the A - B boundary \mathcal{B} .

162 The matrix \mathbf{CF} is a 2-tensor. Theorem 1 states that this tensor can be decomposed into a
 163 TN. We prove it as follows:

164 *Proof (Thm. 1).* Suppose first that control flow in a system A can be represented by a
 165 TN. A TN is, by definition, a factorization of a tensor operator into a network of tensor
 166 operators. This network can be either hierarchical or flat; if it is hierarchical, each layer
 167 can be considered a flat TN. Hence no generality is lost in considering just the case of
 168 a flat TN, which is an operator contraction $T = \dots T_{ij} T_{jk} T_{kl} \dots$, where summation on
 169 shared indices is left implicit. In general, $T_{jk} \neq T_{jk}^T = T_{kj}$, hence these expressions do not
 170 commute. They therefore represent non-trivial control flow. Conversely, any non-trivial
 171 control flow can be written, at any fixed scale or level of abstraction, as a linear sequence
 172 of (in general probabilistic) operators. The fixed order of operators in the sequence can be
 173 encoded formally by adding “spatial” indices as needed to allow contraction over shared
 174 indices. Hence any non-trivial control flow at a fixed scale can be written as a flat TN.
 175 This construction can be repeated at each larger scale to produce a hierarchical TN over a
 176 collection of “lowest-scale” TNs. □

177 We can now examine two corollaries of this result:

178 **Corollary 1.** *Decoherent reference sectors exist on a boundary \mathcal{B} if and only if control*
179 *flow can be implemented by a TN.*

180 *Proof.* Decoherence between sectors requires independently-deployable, non-commuting QRFs.
181 This requires a control structure that factors, hence by Theorem 1, it requires a TN. Con-
182 versely, a TN factors the control structure, making QRFs independently deployable, which
183 renders their sectors decoherent. \square

184 Equivalently, the generative model (GM) implemented by a system [4] factors if, and only
185 if, control flow can be implemented by a TN.

186 **Corollary 2.** *The TN of any system compliant with the FEP is a decomposition of the*
187 *Identity.*

188 *Proof.* The FEP applies to systems with a NESS, and drives such systems to return to (the
189 vicinity of) the NESS after any perturbation. Hence at a sufficiently large scale, the TN of
190 any such system is a cycle, i.e., a decomposition of the Identity. \square

191 Many standard TN models, e.g., MERAs, assume boundary conditions asymptotically far,
192 in numbers of lowest-scale operators, from the region of the network that is of interest.
193 Identifying such asymptotic boundary conditions yields a cyclic system.

194 Theorem 1, together with its corollaries, provides a natural, formal means of classifying
195 systems by their control architectures. At a high level, two characteristics distinguish
196 systems with different architectures:

- 197 • Hierarchical depth, which indicates the number of “virtual machine” layers [43] the
198 architecture supports. The interfaces between these layers implement coarse-graining,

199 removing from the higher-level representation all dimensions, and hence all informa-
 200 tion, which is contracted out of the lower-level operators.

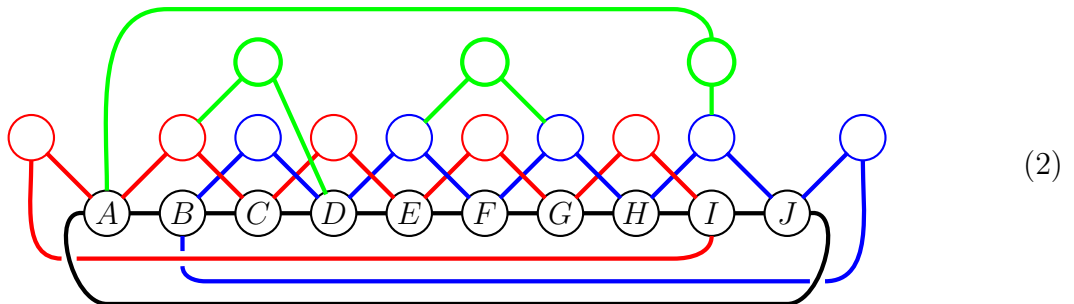
- 201 • Number and location of contractions that yield unitary operators, and hence build in
 202 entanglement between lower-level operators. The natural limit is a MERA, in which
 203 every pair of lower-level operators is entangled at every hierarchical level [44].

204 The control-flow architecture, in turn, specifies the structure of the “layout” of distinguish-
 205 able sectors on \mathcal{B} and hence of detectable features/objects in the environment. Locality on
 206 \mathcal{B} requires a hierarchical TN; detectable entanglement requires a MERA-like TN. Locality
 207 is required for detectable features/objects to appear to have components with nested de-
 208 compositions. Any QRF for geometric space, and hence for spacetime, must be hierarchical,
 209 and must be a MERA if entanglement in space is to be detected. A MERA is required, in
 210 particular, if the use of coherence between spatially-separated systems as a computational
 211 or communication resource is detectable.

212 To illustrate the classification of systems by hierarchical level, consider the ten-step cyclic
 213 TN shown in Diagram (1):



214 and its extension to a hierarchy as shown in Diagram (2):



215 where red, blue, and green colors indicate distinct hierarchical “layers” of tensor contrac-
 216 tions. We have trained artificial neural networks (ANNs) to execute these TNs as the
 217 sequences of state transitions shown in Table 1. The first sequence (Dataset 1) is a ten-step
 218 cycle as shown Diagram (1); the second sequence (Dataset 2) layers the coarse-grained state
 219 transitions of Diagram (2) onto this ten-step cycle. In Dataset 2, a two-bit tag is used to
 220 differentiate the “low-level” from the coarse-grained “high-level” cycles. An example state
 221 state transition from a randomly-generated initial state is shown in Fig. 1; the red-on-green
 222 bit pattern effectively moves “up” one step on each state-transition cycle.

Dataset 1	Dataset 2							
A → B	00	A → B	01	A → C	10	B → D	11	A → D
B → C	00	B → C	01	C → E	10	D → F	11	D → H
C → D	00	C → D	01	E → G	10	F → H	11	H → A
D → E	00	D → E	01	G → I	10	H → J		
E → F	00	E → F	01	I → A	10	J → B		
F → G	00	F → G						
G → H	00	G → H						
H → I	00	H → I						
I → J	00	I → J						
J → A	00	J → A						

223 Table 1: Datasets used in ANN simulations. Dataset 1 specifies a ten-step cycle
 224 $A \rightarrow B \rightarrow \dots \rightarrow J \rightarrow A$. Dataset 2 specifies this same cycle, with three
 225 coarse-grained cycles layered on top. The tags (0,0), (0,1), (1,0), and (1,1)
 226 distinguish the data for the low- and high-level cycles.

227

228

INPUT (T)											OUTPUT (T+1)											
A	1	1	1	0	0	0	1	0	0	1	→	B	1	1	1	0	1	1	1	1	0	1
B	1	1	1	0	1	1	1	1	0	1	→	C	0	1	0	0	1	1	0	0	0	1
C	0	1	0	0	1	1	0	0	0	1	→	D	1	1	1	1	1	0	0	1	0	1
D	1	1	1	1	1	0	0	1	0	1	→	E	1	1	0	0	0	0	0	0	0	1
E	1	1	0	0	0	0	0	0	0	1	→	F	1	1	1	1	0	1	1	0	0	1
F	1	1	1	1	0	1	1	0	0	1	→	G	1	1	1	0	0	1	1	0	1	0
G	1	1	1	0	0	1	1	0	1	0	→	H	0	1	0	1	0	0	0	1	0	1
H	0	1	0	1	0	0	0	1	0	1	→	I	1	0	1	0	0	0	0	1	0	1
I	1	0	1	0	0	0	0	1	0	1	→	J	0	1	1	1	1	1	1	1	0	1
J	0	1	1	1	1	1	1	1	0	1	→	A	1	1	1	0	0	0	1	0	0	1

Figure 1: Example state transition from Dataset 1.

229 We trained two ANNs, one to execute each of the control cycles shown in Table 1. The
230 networks are each composed of three layers, as illustrated in Fig. 2, with network sizes of
231 [10, 50, 10] and [10, 200, 10], respectively, for the input, hidden, and output layers. The
232 units in the hidden layer use the rectified linear unit (ReLU) nonlinear activation function
233 and the neurons in the output layer use the hyperbolic tangent activation function. The
234 network is connected in a feedforward way where a neuron in one layer connects to every
235 neuron in the next layer. Since the ANN serves as a switch state controller, we use a training
236 scheme, similar to one-class classification [45], where the training data are the only data
237 that the network learns to produce. In so doing, the network learns to overfit the training
238 data, and any input outside of the designated state-encoding is discarded. The network
239 is, therefore, not expected to deviate from the learned pattern. The network learns both
240 control regimes with 100% accuracy after training with 3,000 randomly-generated 10-bit
241 inputs.

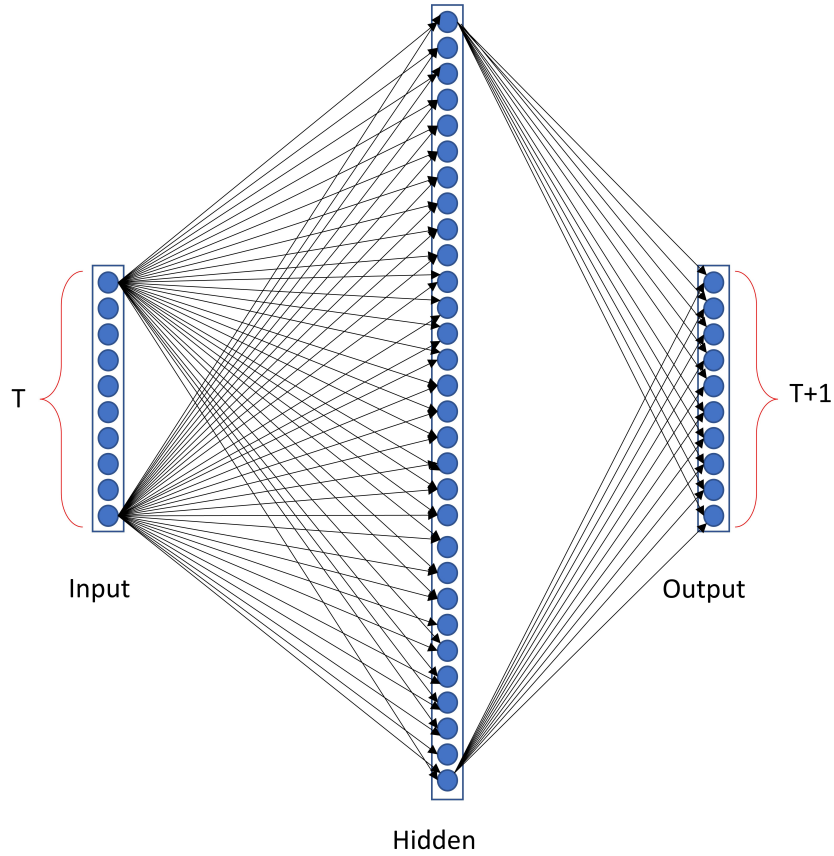


Figure 2: Feed-forward network architecture used to learn the control cycles specified in Table 1. Each node is connected to every node of the next layer, as shown here for the first and last nodes only. The labels ‘T’ and ‘T+1’ indicate time steps in the executed control flow.

242 In the more realistic case of noisy input data, where binary states can be flipped, the
 243 Bidirectional Associative Memory (BAM), a minimal two-layer nonlinear feedback network
 244 [46], is a viable alternative to a shallow feed-forward ANN. The architecture is shown in Fig.
 245 3. This BAM network learns to associate between the two initial and final states in Table
 246 1, with similar performance to that of the feed-forward network.

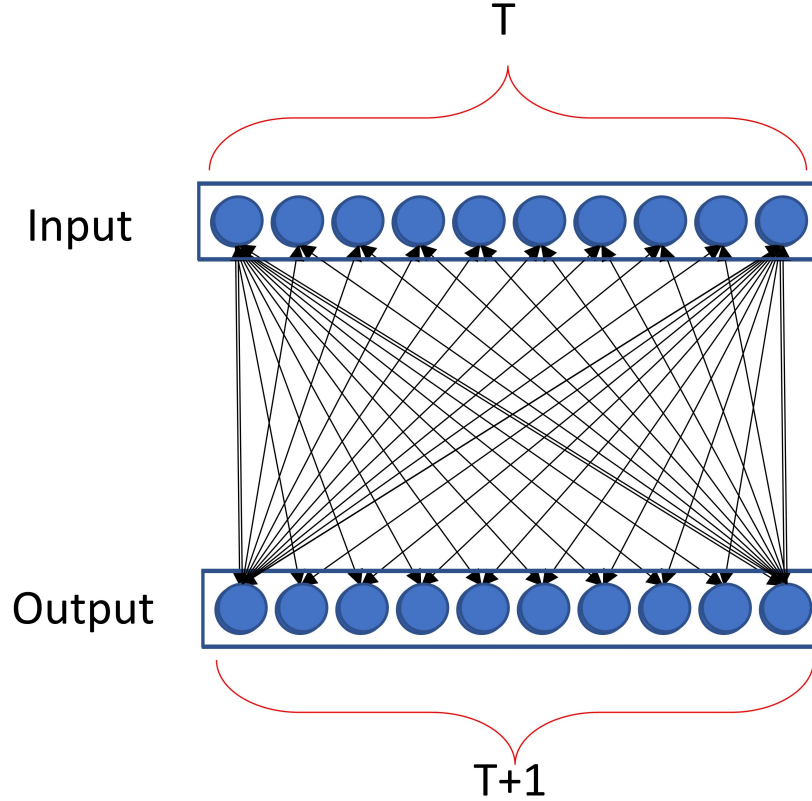


Figure 3: Architecture of the Bidirectional Associative Memory (BAM) network employed here. As in Fig. 2, only the connections of the first and last nodes are shown explicitly.

247 **3 Implementing control flow with TQNNs**

248 Tensor Networks can be naturally associated to the matrix elements of physical scalar
 249 products among topological quantum neural networks (TQNNs). Physical scalar products
 250 encode indeed the dynamics of TQFTs, since they fulfill their constraints of imposing
 251 flatness of the curvature and gauge invariance. Thus, the matrix elements associated to
 252 scalar products can be seen as evolution matrix elements for the spin-network states that
 253 span the Hilbert spaces of TQNNs.

254 3.1 Tensor networks as classifiers for TQNNs

255 A notable example is provided by BF theories [47], a class of TQFTs particularly well
 256 studied in the literature of mathematical physics that enables expressing effective theories
 257 of particle physics, gravity and condensed matter, and provides as well a general frame-
 258 work for implementations of models of quantum information and quantum computation,
 259 machine learning (ML), and neuroscience. These are defined on the principal bundle M of
 260 a connection A for some internal gauge group G , with algebra \mathfrak{g} , according to the action
 261 on a d -dimensional manifold \mathcal{M}_d :

$$\mathcal{S} = \int_{\mathcal{M}_d} \text{Tr}[B \wedge F], \quad (3)$$

262 where B is an $\text{ad}(\mathfrak{g})$ -valued $d-2$ -form, F denotes the field-strength of A , which is a 2-form,
 263 and the trace Tr is over the internal indices of \mathfrak{g} , ensuring gauge invariance of the density
 264 Lagrangian $\mathcal{L} = \text{Tr}[B \wedge F]$ of the BF theory.

265 Variation with respect to the conjugated variables, the connection A and the B frame-field,
 266 closing a canonical symplectic structure, provide the equations of motion of the theory [47]:

$$F = 0, \quad d_A B = 0, \quad (4)$$

267 which are, respectively, the curvature constraint, imposing the flatness of the connection,
 268 and the Gauß constraint, imposing invariance under gauge transformations, having denoted
 269 with d_A the covariant derivative with respect to the connection A .

270 At the quantum level, the states of the kinematical Hilbert space of the theory, fulfilling
 271 by construction the Gauß constraint, can be represented in terms of cylindrical functionals
 272 Cyl , supported on graphs Γ that are unions of segments γ_i , the end points of which meet
 273 in nodes n , and with holonomies – elements of the group G – $H_{\gamma_i}[A]$ of the connection A

274 assigned to γ_i and intertwiner operators – invariant tensor products of representations – v_n
 275 assigned to the nodes n .

276 For $G = \text{SU}(2)$, spin-networks $|\Gamma, j_\gamma, \iota_n\rangle$, supported on Γ and labelled by the spin j_γ of
 277 the irreducible representations of the group elements assigned to γ and by the quantum
 278 intertwiner numbers ι_n associated to v_n , represent a basis of the kinematical Hilbert space
 279 of the theory. In terms of functionals of Cyl , one can provide the holonomy representation,
 280 which is related to the “spin and intertwiner” representation of $|\Gamma, j_\gamma, \iota_n\rangle$ by means of the
 281 Peter-Weyl transform. This allows us to decompose the spin-network cylindric functional
 282 as [48]:

$$\Psi_{j_{\gamma_{ij}}, \iota_{n_i}}(h_{\gamma_{ij}}) = \left(\bigotimes_n \iota_n \right) \cdot \left(\bigotimes_{\gamma_{ij}} D^{(j_{\gamma_{ij}})}(h_{\gamma_{ij}}) \right), \quad (5)$$

283 with $D^{(j)}$ are Wigner matrices providing representation matrices of the $\text{SU}(2)$ group ele-
 284 ments.

285 The functorial evolution among spin-networks is ensured by the projector operator [11],
 286 which implements the curvature constraint in the physical scalar product among states, i.e.

$$\langle \text{in} | P | \text{out} \rangle, \quad \text{with} \quad P = \int \mathcal{D}[N] \exp(\imath \int \text{Tr}[NF]). \quad (6)$$

287 We may then regard $|\text{in}\rangle$ as elements of the Hilbert space, and without loss of generality pick
 288 up those ones resulting from composing tensorially in Cyl k -representations of holonomies.
 289 We may further denote them as $|j_1 \dots j_k\rangle$, with some ordering prescription to associate
 290 the topological structure of Γ to the sequence of spin labels. Physically evolving states
 291 $P|\text{in}\rangle$ are distinguished from the former ones by labelling them as $|\widetilde{j_1 \dots j_k}\rangle$. Similarly, we
 292 introduce $|\text{out}\rangle$ as the tensor product of $(n-k)$ -representations of holonomies, and denote
 293 these states as $|i_1 \dots i_{n-k}\rangle$. Then the matrix elements of $\langle \text{in} | P | \text{out} \rangle$ naturally give rise [27]

294 to an n -tensor, i.e.

$$\langle i_1 \dots i_{n-k} | \widetilde{j_1 \dots j_k} \rangle = T_{i_1 \dots i_{n-k} j_1 \dots j_k} . \quad (7)$$

295 3.2 Geometric RG flow for TQNNs and TNs

296 The mathematical structures of TQNNs we summarized in Sec. 3.1 are picturing systems “at
 297 equilibrium”, for which TQFTs characterize a topological stability that percolates into the
 298 related transition amplitudes. Nonetheless, it is worth considering as well how stochastic
 299 noise might interfere with the topological order ensured by TQFTs, and study the role of
 300 “out-of-equilibrium” physics in the analysis of the evolution of the systems under scrutiny.

301 Out-of-equilibrium dynamics is instantiated considering a heat-flow evolution of the funda-
 302 mental fields of the theory, with respect to a thermal time τ . Typical Langevin equations,
 303 complemented with stochastic noise, provide through their convergence toward the equa-
 304 tions of motion of the theory the relaxation toward equilibrium of the field configurations
 305 representing specific systems [49]. In general, given some fields ϕ_σ , with a classical equation
 306 of motion derived, according to the variational principle $\delta\mathcal{S}/\delta\phi_\sigma$, from an action \mathcal{S} over a
 307 Euclidean manifold \mathcal{M} , the associated Langevin equations read:

$$\frac{\partial}{\partial\tau}\phi_\sigma = -\frac{\delta\mathcal{S}}{\delta\phi_\sigma} + \eta_\sigma , \quad (8)$$

308 with η_σ a stochastic noise term. The theory at equilibrium is characterized by the symme-
 309 tries of the equations of motion $\delta\mathcal{S}/\delta\phi_\sigma = 0$ that are broken in the transient phase [50];
 310 these symmetries are consistent with – and in the case of BF theories, actually generated
 311 by – the theories at equilibrium.

312 A prototype of geometric heat-flow was introduced by Hamilton, and then used by Perelman
 313 to prove the Poincaré conjecture, which goes under the name of Ricci flow. Here the
 314 gravitational field $g_{\mu\nu}$ is the basic configurational space field, while the drift terms are the

315 Einstein equations of motion in the vacuum, which indeed are expressed by requiring that
 316 the components of the Ricci tensor vanish, i.e. $R_{\mu\nu} = 0$. The Ricci flow then reads

$$\iota \frac{\partial}{\partial \tau} g_{\mu\nu} = -2R_{\mu\nu}, \quad (9)$$

317 having considered now a Lorentzian manifold \mathcal{M} . The Ricci flow equations can be further
 318 complemented introducing the Ricci target $R_{\mu\nu}^T = \kappa^2(T_{\mu\nu} - 1/2g_{\mu\nu}T)$, expressed in terms
 319 of the Newton constant $G = \kappa^2/(8\pi)$ and the energy-momentum tensor of matter $T_{\mu\nu}$, so
 320 as to obtain at equilibrium the Einstein equations:

$$R_{\mu\nu} - \frac{1}{2}g_{\mu\nu}R = \kappa^2 T_{\mu\nu}, \quad \text{or equivalently} \quad R_{\mu\nu} = R_{\mu\nu}^T. \quad (10)$$

321 The stochastic version of the Ricci flow, with heat equation turning into a Langevin equa-
 322 tion, has been introduced and deepened in [50] for a generic gravitational system in the
 323 presence of matter fields, describing an action \mathcal{S} for gravity and matter. Moving then from:

$$\iota \frac{\partial}{\partial \tau} g_{\mu\nu} = -\frac{1}{\kappa^2} \frac{\delta \mathcal{S}}{\delta g^{\mu\nu}} + \eta g_{\mu\nu}, \quad (11)$$

324 in which a multiplicative noise $\eta_{\mu\nu} = \eta g_{\mu\nu}$ appears, the Hamiltonian analysis of the stochas-
 325 tic Ricci flow (SRF) in the Adomian decomposition method (ADM) variables has been
 326 derived [50].

327 An essential by-product of the discussion, from the Ricci flow perspective, is that the
 328 equilibration trajectories correspond to those of a renormalization group (RG) flow. The
 329 thermal time τ plays the role of scale parameter that individuates a dimension in the
 330 bulk, which is out-of-equilibrium. The boundaries are recovered asymptotically in τ , in the
 331 infrared regime, and are by definition at equilibrium and thus symmetric.

332 For a particular class of TQFTs, the BF theories we have introduced in Sec. 3.1 for im-

333 plementing TQNNs and TNs, the geometric RG flow acquire a specific expression as the
334 TQFT equivalent of the gravitational Ricci flow [51].

335 **3.3 TNs as a generalization of the main model architectures in** 336 **ML**

337 The use of TNs is an emerging topic in the ML community. The integration between the
338 two appears quite immediate. A TN structure can be viewed as a ML model in which
339 the parameters are properly adjusted to learn the classification of a data set. Yet, as
340 Ref. [52] mentions, machine learning can aid, in turn, in determining a factorization of a
341 TN approximating a data set. Moreover, TNs are also used to compress the layers of ANN
342 architectures, besides a variety of other uses. Tensor networks are becoming more and more
343 popular to the extent that they are a powerful tool for representing and manipulating high-
344 dimensional data, as in the case of image and video classification tasks in which the data
345 are represented as a high-dimensional tensor. High efficiency, flexibility, and ease of use are
346 making them a dominant choice for many AI applications. Furthermore, besides being used
347 to represent data, TNs can be used to process data by exploiting a number of operators.
348 This feature makes them an effective technique for processing data in ML applications.

349 As is well known, TNs are particularly well suited for representing quantum many-body
350 states in which the dimension of the Hilbert space is exponentially large in the number of
351 particles. The corresponding ML approach consists in:

- 352 • Lifting data to exponentially higher spaces;
- 353 • Applying any linear classifier $f(x) = W^* \Phi(X)$ to a non-linear space;
- 354 • Compressing the weights by using TNs.

355 The output of the model is a separation of classes that would not be linearly separable in
 356 a linear space. In particular, the decision function is the overlap of the weight tensor W
 357 with the feature map tensor Φ as in Fig. 4. The weight tensor W can be approximated by
 358 the decomposition in Fig. 5.

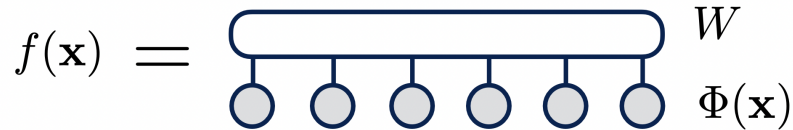


Figure 4: Representation of the decision function (see [53]).

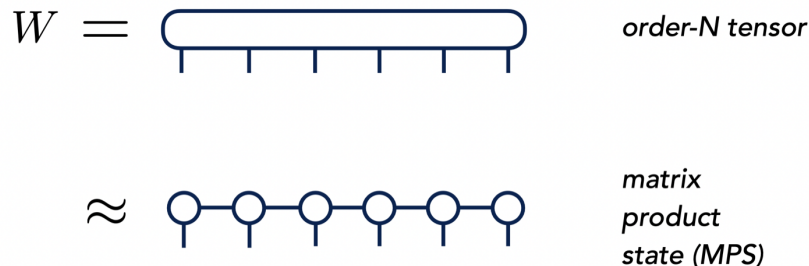


Figure 5: Matrix product decomposition (again see [53]).

359 Regularization and optimization are built as a constructive product of low-order tensors
 360 while weight compression is performed by using the Matrix Product States (MPS) de-
 361 composition. If we look at Deep Neural Networks as a piecewise composition of linear
 362 discriminators (logistic regression functions), then the TN framework appears as a gener-
 363 alization of the main model architectures found in the ML literature, e.g. Support Vector
 364 Machines, Kernel models, and Deep Neural Networks.

365 The literature concerning the use of tensor theory in traditional ML is becoming large. A
 366 short review starts with a seminal paper by Stoudenmire and Schwab [54], which demon-
 367 strated how algorithms for optimizing TNs can be adapted to supervised learning tasks
 368 by using MPS (tensor trains) to parametrize non-linear kernel learning models. Novikov,

369 Trofimov, and Oseledets [55] have shown how an exponentially large tensor of parameters
370 can be represented in a factorized format called Tensor Train (TT), with the consequence
371 of obtaining a regularization of the model. van Glasser, Pancotti, and Cirac [56] explored
372 the connection between TNs and probabilistic graphical models by introducing the concept
373 of a “generalized tensor network architecture” for ML. Ref. [57] then designed a generative
374 model, i.e. a traditional machine learning model that learns joint probability distributions
375 from data and generates samples according to it, by using MPS. Ref. [58] made use of
376 autoregressive MPSs for building an unsupervised learning model that goes beyond proof-
377 of-concept by showing performance comparable to standard traditional models. Finally,
378 Ref. [59] analyzes the contribution of polynomials of different degrees to the supervised
379 learning performance of different architectures.

380 **4 Implications for biological control systems**

381 Scale-free biology requires a smooth transition from quantum-like to classical-like behavior.
382 Typical representations of metabolic, signal-transduction, and gene-regulatory pathways are
383 entirely classical, even though many of their steps involve electron-transfer or other mecha-
384 nisms that are acknowledged to require a quantum-theoretic description [60, 61]. As noted
385 earlier, free-energy budget considerations suggest that both prokaryotic and eukaryotic cells
386 employ quantum coherence as a computational resource [62]. Emerging empirical evidence
387 for longer-range entanglement in mammalian brains suggests that large-scale networks may
388 also be using quantum coherence as a resource [63]. Control flow models must, therefore,
389 support the possibility of quantum computation in biological systems. Hierarchical TNs
390 that include unitary components, e.g., MERA-type models, provide this capability.

391 In prokaryotes, the primary tasks of control flow are adapting metabolism to available
392 resources via metabolite-driven gene regulation [64] and initiating DNA replication and

393 cell division when conditions are favorable. We can, therefore, expect shallow hierar-
394 chies of effectively classical control transitions in these organisms. Eukaryotes, however,
395 are characterized by both intracellular compartmentalization and morphological degrees
396 of freedom at the whole-cell scale. We have shown previously that the FEP will induce
397 “neuromorphic” morphologies – i.e. morphologies that segregate inputs from outputs and
398 enable a fan-in/fan-out computational architecture – in any systems with morphological
399 degrees of freedom [65]. Such systems can be expected to have deep control hierarchies
400 at the cellular level, with hierarchical structure correlating with morphological structure
401 in morphologically-complex cells such as neurons [66], and in multicellular assemblages
402 at all scales. These distinctions correlate with the orders-of-magnitude increase in classi-
403 cal computational power (estimated from total metabolic energy budget) as a function of
404 cell-surface area in eukaryotes as compared to prokaryotes [62], as illustrated in Fig. 6.

405 As well as managing metabolism and replication, most eukaryotes implement active explo-
406 ration of the environment, communication with other systems, and – crucially for cognition
407 – the writing and reading of stigmergic memories. Thus we can expect such systems to im-
408 plement QRFs for spacetime and for specific kinds of objects, e.g., conspecifics and suitable
409 substrates for recording stigmergic memories. Such QRFs rely on symmetries, and hence
410 on redundancy of encoded (or encodable) information; they depend, in other words, on the
411 availability of error-correcting codes [67, 68]. The implementation of spacetime as a QECC
412 by TNs has been extensively studied by physicists as noted above; see [69] for review and
413 [27] for a detailed analysis using the present formalism. The use of spacetime as an error-
414 correcting code by organisms – e.g., the implementation of translational and rotational
415 invariance of objects by dorsal visual processing in mammals [70, 71] – is well-understood
416 phenomenologically, but the details of neural implementation remain to be elucidated.

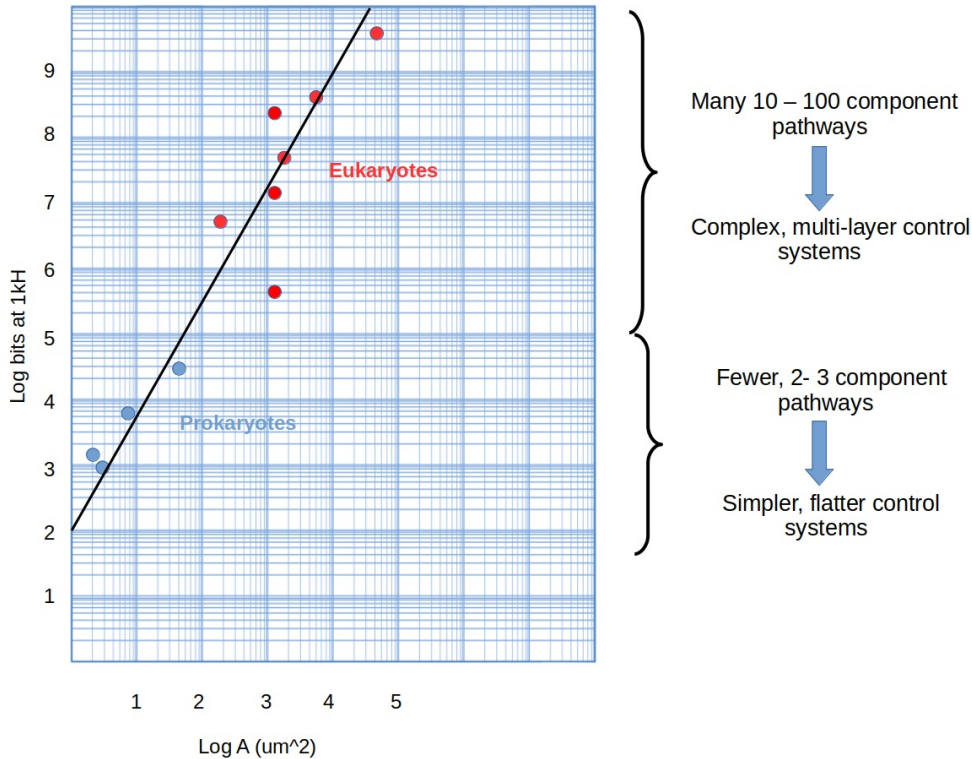


Figure 6: Power-law relation between maximum classical computation rate (vertical axis) and cell-surface area (horizontal axis) derived in [62]. Information processing in eukaryotes is implemented by complex, overlapping signaling pathways that require hierarchical control, which information processing in prokaryotes is implemented by comparatively simple, two or three component pathways that require only shallow control systems. Adapted with permission from [62] Fig. 3.

417 Both the context-sensitivity of, and the occurrence of context effects due to non-commutativity
 418 of QRFs in, control networks can be expected to increase with their complexity and hier-
 419 archical depth. “Bowtie” networks with high fan-in/fan-out to/from multi-use proteins or
 420 second messengers such as Ca^{2+} are increasingly recognized as ubiquitous in higher eu-
 421 karyotic cells [72]. Such networks have the general form of the CCCD depicted in Part I,
 422 Diagram 3. Frequently, such networks evolve via compression of information (e.g. toward
 423 share second messengers, as in $[\text{Ca}^{2+}]$ -based interactions [73, 74]) as an efficiency-increasing

424 mechanism. Bowties introduce semantic ambiguities that must be resolved by context. Each
425 incoming signal has its own governing semantics, but the relevant context can depend on
426 boundary conditions which can be exceedingly difficult (if not impossible) to predetermine
427 (see e.g., [75, 76] for general discussions of the history and semantic depth of this problem).
428 As pointed out in [77], a context change $x \mapsto y$ is semantically problematic if for a fixed
429 set $\{o_i\}$ of observations, the conditional probability distributions $P(o_i|x)$ and $P(o_i|y)$ are
430 well defined, but the joint distribution $P(o_i|x \vee y)$ is not [78]. This occurs whenever the
431 QRFs for x and y do not commute [79, Th 7.1]. As suggested by Part I, Diagram 3, this
432 context-switching problem affects deep learning using VAEs [80]; see e.g., the application
433 to antimicrobial peptides in [81]. In general, the structure of Part I, Diagram 3 can serve as
434 a convenient benchmark for distinguishing signal transduction networks that incorporate
435 co-deployable versus non-co-deployable QRFs [79].

436 “Quantum” context effects due to non-commutativity have, interestingly, been reported
437 even at the scale of human language use. The “Snow Queen” experiment [82] challenged
438 subjects with distinct, mutually-inconsistent meanings of terms such as ‘kind’, ‘evil’, or
439 ‘beautiful’ in different contexts, and detected statistically-significant context effects using
440 the CbD formalism [83, 84]. Such effects cannot be explained by linguistic ambiguity,
441 misreading, etc. Such language-driven contextuality is taken up in the setting of psycholin-
442 guistics and distributional semantics in [85], which combines CbD and the sheaf theoretic
443 [86, 87] methods to systematically study semantic ambiguity as creating meaning/sense
444 discrepancies in statements like “It was about time”, “She had time on her hands to win
445 the heat”, “West led with a queen”, etc.

446 While the notion of “languages” has thus far been applied to cells, tissues, and even non-
447 vertebrates in a mostly metaphorical way, we can speculate that linguistic approaches to
448 understanding the interplay between context dependence and semantic ambiguity may be
449 useful to biology in general. Immune cells (e.g., T cells) are, for example, “programmed” or

450 “trained” by their progenitor cells to respond to local cellular signals and ambient conditions
451 in particular ways. Unexpected context changes may induce dysfunctional (at the organism
452 scale) responses, including chronic disorders [88]; these can be considered consequences of dis-
453 crepancies between the “actual” semantics of incoming signals and the semantics expected
454 by the immune system’s “language.” This suggestion of possible “linguistic” contextuality
455 seems in consonance with the hypothesis of [89] that the immune system is a cognitive (liv-
456 ing) system implementing its exclusive system of language-grammar, which may be prone
457 to analogous disorders of communication as those discussed in [85]. Similar context effects
458 have been observed in microbiological systems [90]; here discrepancies in experimentally
459 derived classical probabilities arising from lactose-glucose interference signaling in *E. Coli*
460 can only be explained in terms of non-classical probabilities. We note that the expression
461 ‘quantum-like’ [91] is often used for such effects; however, their formal structure is exactly
462 that given by quantum theory.

463 We expect that further research into quantum biology will unfold significant perspectives
464 on human/mammalian physiology and cognitive capabilities along the lines suggested in
465 the present article. For example, allostatic maintenance, as briefly alluded to in Part I,
466 can be seen as a process regulating a body’s physiological conditions relative to costs and
467 benefits while dynamically allocating resources for the purpose of overall adaptability of
468 an organism within its internal environment. Implementing the allostatic and anticipatory
469 mechanisms are the visceromotor cortical regions generating autonomic, hormonal, and
470 immunological predictions leading to interoceptive inference [92, 93, 94, 96, 97, 98, 102, 99].
471 This process of inference in humans and mammals putatively utilizes predictive coding for
472 the processes of homeostasis-allostasis through a hierarchy of cellular to organ-level systems,
473 in turn connecting interoception to the processes of exteroception and proprioception
474 [92, 99, 100, 101, 102]. The basic principles follow from how allostasis provides protection
475 against potential surprise by utilizing a framework somewhat beyond the error signaling

476 necessary for homeostatic maintenance (it is essentially through minimizing the free energy
477 of internal state trajectories towards combatting surprise, as discussed in Part I). The
478 net effect of the process is consonant with the Good Regulator theorem of [95], showing
479 how regulation of a given system requires an internal model of that system. A further
480 perspective is to emphasize the predictive nature of an integrated, complex, allostatic-
481 interoceptive cortical system capable of supporting a spectrum of psychological phenomena
482 including memory and emotions [99] (cf. [102]). Accordingly, cognitive conditions such
483 as depression and autism have been described as abnormalities of allostatic-interoceptive
484 inference, so impairing predictive coding mechanisms due to aberrant assimilation and
485 mistuning of prediction errors (putatively a connectivity issue), conceivably leading to a
486 root cause of many known cognitive conditions [92, 100, 102].

487 We anticipate that this fully general, context sensitive model of control flow will be im-
488 portant for understanding morphogenesis, which is not simply a feed-forward emergent
489 system, but rather a highly context-sensitive error-minimizing process [103]. Specifically,
490 the collective intelligence of cells during embryonic development, organ regeneration, and
491 metamorphosis can create and repair specific complex structures despite a wide range of
492 perturbations [104]. Changes in the genome, the number of cells, or the starting configura-
493 tion can often be overcome: bisected embryos result in normal twins, amputated salamander
494 limbs re-grow back to normal, and planarian fragments result in perfect little worms [105].
495 The competency of cellular collectives to reach the correct target morphology despite even
496 drastic interventions requires an understanding of how they navigate, via context-sensitive
497 control flow, problem spaces including anatomical morphospace [106], physiological, and
498 transcriptional spaces [68, 107]. Understanding the navigation policies used by unconven-
499 tional collective intelligences can help not only understand creative problem-solving on rapid
500 timescales (such as the ability to regulate genes to accommodate an entirely novel stressor
501 [108] without evolutionary adaptation), but may also have implications for predicting and

502 managing the goals and behavioral repertoires of synthetic beings [109].

503 **5 Conclusion**

504 We have shown here how the problem of defining control flow arises in active inference
505 systems, and provided three formal representations of the problem. We have proved that
506 control flow in such systems can always be represented by a tensor network, provided
507 illustrative examples, and shown how the general formalism of topological quantum neural
508 networks can be used to implement a general model of control flow. These results provide
509 a general formalism with which to characterize context dependence in active inference
510 systems at any scale, from that of macromolecular pathways to that of multi-organism
511 communities. They suggest that the concept of communication by language is not just
512 metaphorical when applied to biological systems in general, but rather an appropriate and
513 productive description of interactional dynamics.

514 We view these results as a further step toward fully integrating the formal models, concepts,
515 and languages of physics, biology, and cognitive science. This integration is not reductive.
516 It rather allows us to classify systems using natural measures of organizational and com-
517 putational complexity, and to understand how interactions between simpler systems can
518 implement the more complex behavior of the larger systems that they compose.

519 **Acknowledgements**

520 K.F. is supported by funding for the Wellcome Centre for Human Neuroimaging (Ref:
521 205103/Z/16/Z), a Canada-UK Artificial Intelligence Initiative (Ref: ES/T01279X/1) and
522 the European Union’s Horizon 2020 Framework Programme for Research and Innovation

523 under the Specific Grant Agreement No. 945539 (Human Brain Project SGA3). M.L. grate-
524 fully acknowledges funding from the Guy Foundation and the John Templeton Foundation,
525 Grant 62230. A.M. wishes to acknowledge support by the Shanghai Municipality, through
526 the grant No. KBH1512299, by Fudan University, through the grant No. JJH1512105,
527 the Natural Science Foundation of China, through the grant No. 11875113, and by the
528 Department of Physics at Fudan University, through the grant No. IDH1512092/001.

529 Conflict of interest

530 The authors declare no competing, financial, or commercial interests in this research.

531 References

- 532 [1] Friston, K. J. 2010 The free-energy principle: A unified brain theory? *Nature Reviews*
533 *Neuroscience* 11, 127–138.
- 534 [2] Friston, K. J. 2013 Life as we know it. *Journal of The Royal Society Interface* 10,
535 20130475.
- 536 [3] Friston KJ, FitzGerald T, Rigoli F, Schwartenbeck P, Pezzulo G. Active inference: a
537 process theory. *Neural Comput* 2017;29:1–49.
- 538 [4] Friston, K. J. 2019 A free energy principle for a particular physics. Preprint
539 arxiv:1906.10184 [q-bio.NC]. <https://arxiv.org/abs/1906.10184>
- 540 [5] Ramstead MJ, Sakthivadivel DAR, Heins C, Koudahl M, Millidge B, Da Costa L,
541 Klein B, Friston KJ 2022 On Bayesian mechanics: A physics of and by beliefs. *Inter-*
542 *face Focus* 13, 2022.0029.

- 543 [6] Fields C, Friston K, Glazebrook JF, Levin M 2022 A free energy principle for generic
544 quantum systems. *Prog. Biophys. Mol. Biol.* 173, 36–59.
- 545 [7] Friston, K., Da Costa, L., Sakthivadivel, D. A. R., Heins, C., Pavliotis, G. A., Ram-
546 stead, M., Parr, T. 2022 Path integrals, particular kinds, and strange things. Preprint
547 arxiv:2210.12761.
- 548 [8] Aharonov Y, Kaufherr T. Quantum frames of reference. *Phys Rev D* 1984;30:368–385.
- 549 [9] Bartlett SD, Rudolph T, Spekkens RW. 2007 Reference frames, super-selection rules,
550 and quantum information. *Rev Mod Phys* 79, 555–609.
- 551 [10] Atiyah, M. 1988 Topological quantum field theory. *Pub. Math. IHÈS* 68, 175–186.
- 552 [11] Fields, C.; Glazebrook, J. F.; Marcianò, A. (2022) Sequential measurements, topo-
553 logical quantum field theories, and topological quantum neural networks. *Fortschr.*
554 *Phys.* 2022, 2200104.
- 555 [12] Marcianò, A.; Chen, D.; Fabrocini, F.; Fields, C.; Greco, E.; Gresnigt, N.; Jinklub,
556 K.; Lulli, M., Terzidis, K.; Zappala, E. 2022 Quantum neural networks and topological
557 quantum field theories. *Neural Networks* 153, 164–178.
- 558 [13] Marcianò, A., Chen, D., Fabrocini, F., Fields, C., Lulli, M., Zappala, E. 2022 Deep
559 neural networks as the semi-classical Limit of topological quantum neural networks:
560 The problem of generalisation. Preprint arXiv:2210.13741.
- 561 [14] Qi, X.-L. Does gravity come from quantum information? *Nature Phys.* 14, 984-987
562 (2018), <https://doi.org/10.1038/s41567-018-0297-3>.
- 563 [15] Bekenstein, J. D. Black holes and the second law. *Lett. Nuovo Cim.* 4, 737-740 (1972).
- 564 [16] Bekenstein, J. D. Black holes and entropy. *Phys. Rev. D* 7, 2333-2346 (1973).

- 565 [17] Hawking, S. W. Gravitational radiation from colliding black holes. *Phys. Rev. Lett.*
566 26, 1344-1346 (1971).
- 567 [18] Hawking, S. W. Black hole explosions? *Nature* 248, 30-31 (1974).
- 568 [19] Susskind, L. The world as a hologram. *J. Math. Phys.* 36, 6377-6396 (1995).
- 569 [20] Bousso, R. The holographic principle. *Rev. Mod. Phys.* 74, 825-874 (2002).
- 570 [21] 't Hooft, G. Dimensional reduction in quantum gravity. Preprint at
571 <https://arxiv.org/abs/gr-qc/9310026> (1993).
- 572 [22] Maldacena, J. The large-N limit of superconformal field theories and supergravity.
573 *Int. J. Theor. Phys.* 38, 1113 (1999).
- 574 [23] Ryu, S. and Takayanagi, T. Holographic derivation of entanglement entropy from
575 AdS/CFT, *Phys. Rev. Lett.* 96, 181602 (2006).
- 576 [24] Almheiri, A., Dong, X. and Harlow, D. Bulk locality and quantum error correction
577 in AdS/CFT. *J. High Energy Phys.* 2015, 163 (2015).
- 578 [25] Hubeny, V. E. and Rangamani, M. Causal holographic information. *J. High Energy*
579 *Phys.* 2012, 114 (2012).
- 580 [26] Headrick, M., Hubeny, V. E., Lawrence, A. and Rangamani, M. Causality and holo-
581 graphic entanglement entropy. *J. High Energy Phys.* 2014, 162 (2014).
- 582 [27] Fields, C.; Glazebrook, J. F.; Marcianò, A. 2023 Communication protocols and quan-
583 tum error-correcting codes from the perspective of topological quantum field theory.
584 Preprint arxiv:2303.16461 [hep-th].
- 585 [28] Swingle, B. Entanglement renormalization and holography. *Phys. Rev. D* 86, 065007
586 (2012).

- 587 [29] White, S. R. Density matrix formulation for quantum renormalization groups. *Phys.*
588 *Rev. Lett.* 69, 2863-2866 (1992).
- 589 [30] Verstraete, F., Murg, V. and Cirac, J. I. Matrix product states, projected entangled
590 pair states, and variational renormalization group methods for quantum spin systems.
591 *Adv. Phys.* 57, 143-224 (2008).
- 592 [31] DiVincenzo, D. P. et al. in *Quantum Computing and Quantum Communications* (ed.
593 Williams, C. P.) 247-257 (Springer, Berlin, 1999).
- 594 [32] Vidal, G. Class of quantum many-body states that can be efficiently simulated. *Phys.*
595 *Rev. Lett.* 101, 110501 (2008).
- 596 [33] Pastawski, F., Yoshida, B., Harlow, D. and Preskill, J. Holographic quantum error-
597 correcting codes: toy models for the bulk/boundary correspondence. *J. High Energy*
598 *Phys.* 2015, 149 (2015).
- 599 [34] Yang, Z., Hayden, P. and Qi, X.-L. Bidirectional holographic codes and sub-AdS
600 locality. *J. High Energy Phys.* 2016, 175 (2016).
- 601 [35] Hayden, P. et al. Holographic duality from random tensor networks. *J. High Energy*
602 *Phys.* 2016, 9 (2016).
- 603 [36] Han, M. and Huang, S. Discrete gravity on random tensor network and holographic
604 Rényi entropy. *J. High Energy Phys.* 2017, 148 (2017).
- 605 [37] Lashkari, N., McDermott, M. B. and Van Raamsdonk, M. Gravitational dynamics
606 from entanglement “thermodynamics”. *J. High Energy Phys.* 2014, 195 (2014).
- 607 [38] Swingle, B. and Van Raamsdonk, M. Universality of gravity from entanglement.
608 Preprint at <https://arxiv.org/abs/1405.2933> (2014).

- 609 [39] Shenker, S. H. and Stanford, D. Black holes and the butterfly effect. *J. High Energy*
610 *Phys.* 2014, 67 (2014).
- 611 [40] Sachdev, S. and Ye, J. Gapless spin-fluid ground state in a random quantum Heisen-
612 berg magnet. *Phys. Rev. Lett.* 70, 3339-3342 (1993).
- 613 [41] Kitaev, A. A simple model of quantum holography. KITP <http://online.kitp.>
614 [ucsb.edu/online/entangled15/kitaev/](http://online.kitp.ucsb.edu/online/entangled15/kitaev/); [http://online.kitp.ucsb.edu/online/entan-](http://online.kitp.ucsb.edu/online/entangled15/kitaev2/)
615 [gled15/kitaev2/](http://online.kitp.ucsb.edu/online/entangled15/kitaev2/) (2015).
- 616 [42] Maldacena, J. and Stanford, D. Remarks on the Sachdev-Ye-Kitaev model. *Phys.*
617 *Rev. D* 94, 106002 (2016).
- 618 [43] Smith, J. E., Nair, R. 2005 The architecture of virtual machines. *IEEE Computer*
619 38(5), 32–38.
- 620 [44] Orús, R. 2019 Tensor networks for complex quantum systems. *Nat. Rev. Phys.* 1,
621 538–550.
- 622 [45] Manevitz, L. M., Yousef, M. 2002 One-class SVMs for document classification. *J.*
623 *Mach. Learn. Res.* 2, 139–154.
- 624 [46] Kosko, B. 1988 Bidirectional associative memories. *IEEE Trans. Syst. Man Cybern.*
625 18, 49–60.
- 626 [47] J. Baez, Four-dimensional BF theory as a topological quantum field theory *Lett. Math.*
627 *Phys.* 1996, 38, 129.
- 628 [48] Rovelli, C. *Quantum Gravity*, Cambridge University Press, Cambridge, UK 2004.
- 629 [49] Parisi, G. and Wu, Y.-S. Perturbation theory without gauge fix-
630 ing, *Scientia Sinica* 24, 483 (1981); doi: 10.1360/ya1981-24-4-483,
631 <http://engine.scichina.com/doi/10.1360/ya1981-24-4-483>.

- 632 [50] Lulli, M., Marcianò, A. and Shan, X. Stochastic Quantization of General Relativity
633 à la Ricci-Flow, [arXiv:2112.01490 [gr-qc]].
- 634 [51] Marcianò, A. *in preparation*.
- 635 [52] Sengupta, R. Adhikary, S. Oseledets, I. and Biamonte, J. Tensor Networks in Machine
636 Learning, <https://arxiv.org/pdf/2207.02851.pdf>, 2022.
- 637 [53] E. Miles Stoudenmire, Talk at the International Center for Theoretical Physics Tri-
638 este, August 2018.
- 639 [54] Stoudenmire, E.M. Schwab, D.J. Supervised Learning with Quantum-Inspired Tensor
640 Networks, <https://arxiv.org/abs/1605.05775>, 2016.
- 641 [55] Novikof, A. Trofimov, M. and Oseledets, I. Exponential Machines,
642 <https://arxiv.org/abs/1605.03795>, 2017.
- 643 [56] Glasser, I. Pancotti, N. and Cirac, J.I. From probabilistic graphical models to gen-
644 eralized tensor networks for supervised learning, <https://arxiv.org/abs/1806.05964>,
645 2018.
- 646 [57] Han, Z.-H. Wang, J. Fan, H. Wang, L. and Zhang, P. Unsupervised Generative Mod-
647 eling Using Matrix Product States, *Physical Review X*, 8, 2018.
- 648 [58] Liu, J. Li, S.-J. Zhang, J. and Zhang, P. Tensor networks for unsupervised machine
649 learning, <https://arxiv.org/abs/2106.12974>, 2021.
- 650 [59] Convy, I. and Whaley, K.B. Interaction Decompositions for Tensor Network Regres-
651 sion, <https://arxiv.org/abs/2208.06029>, 2022.
- 652 [60] Zweir MC, Chong LT. 2010 Reaching biological timescales with all-atom molecular
653 dynamics simulations. *Curr. Opin. Pharmacol.* 10: 745–752.

- 654 [61] Groenhof, G. 2013 Introduction to QM/MM simulations. *Methods Mol. Biol.* 924,
655 43–66.
- 656 [62] Fields, C.; Levin, M. 2021 Metabolic limits on classical information processing by
657 biological cells. *BioSystems* 209, 104513.
- 658 [63] Kerskens, C. M., Pérez, D. L. 2022 Experimental indications of non-classical brain
659 functions. *J. Phys. Commun.* 6, 105001.
- 660 [64] Ledezma-Tejeida, D.; Schastnaya, E.; Sauer, U. 2021 Metabolism as a signal generator
661 in bacteria. *Curr. Opin. Syst. Biol.* 28, 100404.
- 662 [65] Fields, C.; Friston, K.; Glazebrook, J. F.; Levin, M.; Marcianò, A. 2022 The free
663 energy principle induces neuromorphic development. *Neuromorph. Comp. Engin.* 2,
664 042002.
- 665 [66] Fields, C.; Glazebrook, J. F.; Levin, M. 2022 Neurons as hierarchies of quantum
666 reference frames. *Biosystems* 219, 104714.
- 667 [67] Fields, C.; Levin, M. 2018 Multiscale memory and bioelectric error correction in the
668 cytoplasm-cytoskeleton-membrane system. *WIREs Syst. Biol. Med.* 10, e1410.
- 669 [68] Fields, C., Levin, M. 2022 Competency in navigating arbitrary spaces as an invariant
670 for analyzing cognition in diverse embodiments. *Entropy* 24, 819.
- 671 [69] Bain, J. 2020 Spacetime as a quantum error-correcting code? *Stud. Hist. Phil. Mod.*
672 *Phys.* 71, 26–36.
- 673 [70] Flombaum, J. I.; Scholl, B. J.; Santos, L. R. 2008 Spatiotemporal priority as a fun-
674 damental principle of object persistence. In: *The Origins of Object Knowledge*, eds
675 B. Hood and L. Santos (Oxford: Oxford University Press), 135–164.

- 676 [71] Fields, C. 2011 Trajectory recognition as the basis for object individuation: A func-
677 tional model of object file instantiation and object-token encoding. *Front. Psychol.* 2,
678 49.
- 679 [72] Niss, K.; Gomez-Casado, C.; Hjaltelin, J. X.; Joeris, T.; Agace, W. W.; Belling, K.
680 G.; Brunak, S. 2020 Complete topological mapping of a cellular protein interactome
681 reveals bow-tie motifs as ubiquitous connectors of protein complexes. *Cell Rep.* 31,
682 107763.
- 683 [73] Carafoli, E. and Krebs, J. Why calcium? How calcium became the best communica-
684 tor. *J. Biol Chem* 40 2016, 20849–20857.
- 685 [74] Polouliakh, N., Nock, R., Nielsen, F. and Kitano, H. G-protein coupled receptor
686 signaling architecture of mammalian immune cells. *PLoS ONE* 4(1) 2009, e4189.
- 687 [75] Friedlander, T., Mayo, A. E., Thlusty, T. and Alon, U. Evolution of bow-tie architec-
688 tures in biology. *PLOS Computational Biology* 11(3) 2015, e1004055
- 689 [76] Boniolo, G., D’Agostino, M., Piazza, M. and Pulcini, G. Molecular biology
690 meets logic: Context-sensitivity in focus. *Foundations of Science* 2021 in press,
691 <https://doi.org/10.1007/s10699-021-09789-y>
- 692 [77] Fields, C.; Glazebrook, J. F.; Levin, M. 2021 Minimal physicalism as a scale-free
693 substrate for cognition and consciousness. *Neurosci. Cons.* 7(2), niab013.
- 694 [78] Kochen, S., Specker, E. P. 1967 The problem of hidden variables in quantum mechan-
695 ics. *J. Math. Mech.* 17, 59–87.
- 696 [79] Fields, C.; Glazebrook, J. F. 2022 Information flow in context-dependent hierarchical
697 Bayesian inference. *J. Expt. Theor. Artif. intell.* 34, 111–142.

- 698 [80] Kingma, D. P and Welling, M. An Introduction to variational autoencoders. *Foundations and Trends in Machine Learning* 12(4) (2019), 307–392.
699
- 700 [81] Dean, S. N. and Walper, S. A. Variational autoencoder for generation of antimicrobial peptides. *ACS Omega* 5 2020, 20746–20754.
701
- 702 [82] Cervantes, V. H., Dzhafarov, E. N. (2018). Snow Queen is evil and beautiful: Experimental evidence for probabilistic contextuality in human choices. *Decision* 5(3),
703 193–204.
704
- 705 [83] Dzhafarov, E. N.; Kujala, J. V. (2017a). Contextuality-by-Default 2.0: Systems with
706 binary random variables. In: J. A. Barros, B. Coecke and E. Pothos (eds.) *Lecture Notes in Computer Science* 10106, Springer, Berlin, 16–32.
707
- 708 [84] Dzhafarov, E. N. & Kon, M. 2018 On universality of classical probability with contextually labeled random variables. *J. Math. Psychol.* 85, 17–24.
709
- 710 [85] Wang, D., Sadrzadeh, Abramsky, S. and Cervantes, V. H. On the quantum-like contextuality of ambiguous phrases. *Proceedings of the 2021 Workshop on Semantic Spaces at the Intersection of NLP, Physics and Cognitive Science*, pp. 42–52. Association for Computational Linguistics 2021.
711
712
713
- 714 [86] Abramsky, S., Brandenburger, A. 2011 The sheaf-theoretic structure of non-locality and contextuality. *New J. Phys.* 13, 113036.
715
- 716 [87] Abramsky, S., Barbosa, R. S., Mansfield, S. 2017 Contextual fraction as a measure of contextuality. *Phys. Rev. Lett.* 119, 050504.
717
- 718 [88] Editorial Focus. 2019 A matter of context. *Nature Immunol.* 20, 769.
- 719 [89] Atlan, H. and Cohen, I. R. 1998 Immune information, self-organization and meaning. *Int. Immunology* 10, 711–717.
720

- 721 [90] Basieva I, Khrennikov A, Ohya M, Yamato O. Quantum-like interference effect in gene
722 expression: glucose-lactose destructive interference. *Syst Synth Biol* 2011;5:59–68.
- 723 [91] Khrennikov, A. Quantum-like modeling of cognition. *Front Phys* 3 2015:77.
- 724 [92] Barrett, L. F., and Simmons, W. K. (2015) Interoceptive predictions in the brain.
725 *Nat. Rev. Neurosci.* **16**(7): 419–429.
- 726 [93] Barrett, L. F., Quigley, K. S. and Hamilton, P. An active inference theory of allostasis
727 and interoception in depression. *Phil. Trans. R. Soc. B* 371: 20160011.
- 728 [94] Barrett, L. F. The theory of constructed emotion: an active inference account of
729 interoception and categorization. *Soc. Cogn. Affect. Neurosci.* 12 2017, 1–23.
- 730 [95] Conant RC, Ashby WR. Every good regulator of a system must be a model of that
731 system. *Int. J. Syst. Sci.* 1970;1(2):89–97.
- 732 [96] Corcoran, A. W., Pezzulo, G., Hohwy, J. 2020 From allostatic agents to counterfactual
733 cognisers: Active inference, biological regulation, and the origins of cognition. *Biol.*
734 *Philos.* 35(3), 32.
- 735 [97] Hohwy, J. *The Predictive Mind*. Oxford University Press, Oxford, UK, 2013
- 736 [98] Hohwy, J. 2016 The self-evidencing brain. *Nouûs* 50(2), 259–285.
- 737 [99] Kleckner, I. R. et al. Evidence for a large-scale brain system supporting allostasis and
738 interoception in humans. *Nature Human Behaviour* 11 2017, Article 0069, 14 pages.
- 739 [100] Seth, A. K., Suzuki, K, and Critchley, H. D. An interoceptive predictive coding model
740 of conscious presence. *Frontiers in Psychology* 2 Article 395, 16 pages.
- 741 [101] Seth, A. K. (2013) Interoceptive inference, emotion, and the embodied self. *Trends*
742 *in Cognitive Science* **17** (11): 565–573.

- 743 [102] Seth, A. K. and Friston, K. J. Active interoceptive inference and the emotional
744 brain. *Phil. Trans. R. Soc. B* 371, 20160007.
- 745 [103] Levin, M. 2022 Technological approach to mind everywhere: An experimentally-
746 grounded framework for understanding diverse bodies and minds. *Front. Syst. Neu-*
747 *rosci.* 16, 768201.
- 748 [104] Pezzulo, G., Levin, M. 2016 Top-down models in biology: explanation and control
749 of complex living systems above the molecular level. *J. R. Soc. Interface* 13(124),
750 20160555.
- 751 [105] Birnbaum, K. D., Sánchez Alvarado, A. 2008 Slicing across kingdoms: Regeneration
752 in plants and animals. *Cell* 132(4), 697–710.
- 753 [106] Levin, M. 2022 Collective intelligence of morphogenesis as a teleonomic process.
754 Preprint PsyArXiv hqc9b.
- 755 [107] Biswas, S., Clawson, W., Levin, M. 2023 Learning in transcriptional network models:
756 Computational discovery of pathway-level memory and effective interventions. *int. J.*
757 *Molec. Sci.* 24(1), 285.
- 758 [108] Emmons-Bell, M., Durant, F., Tung, A. et al. 2019 Regenerative adaptation to elec-
759 trochemical perturbation in planaria: A molecular analysis of physiological plasticity.
760 *iScience* 22, 147–165.
- 761 [109] Clawson, W., Levin, M. 2022 Endless forms most beautiful 2.0: Teleonomy and the
762 bioengineering of chimaeric and synthetic organisms. *Biol. J. Linnean Soc.* 2022,
763 blac073.